



# Manganese tolerance in *Verbascum olympicum* Boiss. affecting elemental uptake and distribution: changes in nicotinic acid levels under stress conditions

Umran Seven Erdemir<sup>1</sup> · Hulya Arslan<sup>2</sup> · Gurcan Guleryuz<sup>2</sup> · Mehmet Yaman<sup>3</sup> · Seref Gucer<sup>1</sup>

Received: 9 March 2018 / Accepted: 6 August 2018 / Published online: 15 August 2018  
© Springer-Verlag GmbH Germany, part of Springer Nature 2018

## Abstract

A multielemental determination methodology in conjunction with an organic acid analysis that were supplemented with other stress parameters and an ultrastructural analysis used herein to study *Verbascum olympicum* Boiss. (Scrophulariaceae) under Mn stress. Uptake and accumulation characteristics of B, Cu, Fe, Mn, Mo, and Zn were evaluated in 8-week-old seedlings grown in Hoagland's nutrient solution and exposed to 5 (CK), 50, and 200  $\mu\text{M}$   $\text{MnSO}_4$  for 7 days. Hydrogen peroxide levels were determined to evaluate oxidative stress, and changes in compatible substance levels (total phenolic contents, glutathione and glutathione disulfide levels) were determined to assess antioxidant defense mechanisms. The distribution of manganese on the root surface was characterized by scanning electron microscopy images and energy-dispersive X-ray spectroscopy analysis. The levels of nicotinic acid, which is involved in nicotinamide adenine dinucleotide biosynthesis, were determined in roots and leaves to assess tolerance mechanisms. *V. olympicum* exhibited the ability to cope with oxidative stress originating from excessive Mn, while increased Mn concentrations were observed in both roots and leaves. The translocation factor of B was the most affected among other studied elements under the experimental conditions. Total nicotinic acid levels exhibited a trend of reduction in the roots and leaves, which could be attributed to the appropriate metabolic progress associated with oxidative stress based on the nicotinamide adenine dinucleotide cycle that may reach glutathione in response to manganese stress during plant growth.

**Keywords** *Verbascum olympicum* Boiss. · Manganese stress · Element uptake · Hydrogen peroxide · Total nicotinic acid

## Introduction

Manganese (Mn) is important in photosynthesis, in which a cluster of Mn atoms is required as the catalytic center for light-

induced water oxidation in photosystem II, and it has an important role as a cofactor for a variety of enzymes, such as  $\text{Mn}^{2+}$ -dependent superoxide dismutase (MnSOD), which protects plants against reactive oxygen species (Marschner 1995).

Plants uptake manganese as the divalent cation  $\text{Mn}^{2+}$  via an active transport system in epidermal root cells (Marschner 1995). Plant Mn requirements are generally low, and although the critical deficiency level was reported to be 10–20  $\mu\text{g g}^{-1}$  (Kramer 2010), Mn concentrations in excess of critical levels of 200–3500  $\mu\text{g g}^{-1}$  can be toxic to plants. Growth retardation, brown lesions, foliar chlorosis, and crinkled leaves are the main symptoms of manganese toxicity (Petolino and Collins 1985). These symptoms are related to other metabolic processes, such as photosynthesis and respiration (Macfie and Taylor 1992). Suppressed biomass, problems with photosynthesis, and induced biochemical disorders, such as oxidative stress, are caused by Mn phytotoxicity (Millaleo et al. 2010). Manganese-induced oxidative stress has been described in numerous plants, such as barley (Demirevska-Kepova et al.

---

Responsible editor: Philippe Garrigues

**Electronic supplementary material** The online version of this article (<https://doi.org/10.1007/s11356-018-2924-z>) contains supplementary material, which is available to authorized users.

✉ Umran Seven Erdemir  
useven@uludag.edu.tr

<sup>1</sup> Department of Chemistry, Faculty of Arts and Sciences, Bursa Uludag University, Bursa, Turkey

<sup>2</sup> Department of Biology, Faculty of Arts and Sciences, Bursa Uludag University, Bursa, Turkey

<sup>3</sup> Department of Chemistry, Faculty of Science, Firat University, Elazig, Turkey

2004) and *Cucumis sativus* (Shi et al. 2005), and *Polygonum perfoliatum* L. is highlighted as an example of an Mn-tolerant plant given its minimal ultrastructural changes in response to oxidative stress (Xue et al. 2018). Excess Mn may also alter nutritional transactions between minerals in plants; high Mn levels may disrupt nutrient balances by interacting with other elements, especially divalent cations such as magnesium, calcium, and zinc (de Varennes et al. 2001).

Plants have mechanisms to cope with the toxic effects of heavy metals, such as the biosynthesis of metal-binding peptides and phytochelatins (Martinez et al. 2006). Within this context, molecules that may function as potential defense agents include ascorbate, glutathione (GSH), phenolic compounds, alkaloids,  $\alpha$ -tocopherols, and superoxide dismutase, and these molecules are examples of enzymatic and non-enzymatic antioxidants or non-protein amino acids (Rahman et al. 2016). Furthermore, nicotinamide adenine dinucleotide (NAD) and its phosphate derivative NADP are important metabolites that allow plants to adapt and survive under numerous environmental stresses (Hashida et al. 2009). The exposure of plant cells to oxidative stress reduces overall levels of NAD, which is involved in photosynthesis and plant stress responses (Noctor et al. 2006; Smith et al. 2010). Phosphorylated forms of NAD (NADP<sup>+</sup>/NADPH) are important for regenerating oxidative defense metabolism (Bornhorst et al. 2012), and NADP is formed from NAD in a specific pathway that produces GSH via the ascorbate-glutathione cycle (Foyer and Noctor 2011; Smith et al. 2010). The important role of GSH appears to involve an antioxidative plant defense mechanism for scavenging reactive oxygen species under oxidative stress conditions (Syta et al. 2013). Moreover, nicotinamide, and its natural metabolite nicotinic acid in NAD cycle, and GSH, were also identified in earlier studies as having the ability to induce metal tolerance or being connected to the oxidative stress mechanisms of plants. These metabolites increase GSH levels by inducing defense metabolism in plant cells (Berglund 1994; Berglund and Ohlsson 1995; Ohlsson et al. 2008), and one of the significant roles of the elements in this context is that metalloids may affect the cellular levels of single adenine and/or pyridine nucleotides (Bornhorst et al. 2012). NAD formation in the presence of activating cations, such as Cd<sup>2+</sup>, Mn<sup>2+</sup>, Mg<sup>2+</sup>, Zn<sup>2+</sup>, Co<sup>2+</sup>, and Ni<sup>2+</sup>, has been described. The requirement for Mg<sup>2+</sup> or Mn<sup>2+</sup> in the catalysis of NAD formation has been reported in pig liver (Jackson and Atkinson 1966). Although NAD recycling is different in plants and mammals (Hashida et al. 2009), between 50 and 500  $\mu$ M MnCl<sub>2</sub> are required to reduce cellular levels of nicotinamide adenine dinucleotides (NAD<sup>+</sup> and NADH) or the NAD<sup>+</sup>/NADH ratio in human lung cells with significant effects starting at 50  $\mu$ M (NAD<sup>+</sup>) and 250  $\mu$ M (NADH) MnCl<sub>2</sub> (Bornhorst et al. 2012).

Given the relationships between the elements and NAD, Mn and Mg stimulate nicotinamidase activity by 1.3-fold

and 1.7-fold, respectively, whereas many of the other elements exhibit strong inhibitory (Zn<sup>2+</sup>, Cu<sup>2+</sup>, Fe<sup>2+</sup>, and Fe<sup>3+</sup>) or no inhibitory (Na<sup>+</sup>, K<sup>+</sup>, and Ca<sup>2+</sup>) effects (Wang and Pichersky 2007). In connection with Mn, NAD has been shown to play a preventative role against Mn-induced degenerative metabolic loss due to high Mn exposure in animal studies. The inhibitory effect of Mn on oxidative phosphorylation has been described (Wang et al. 2014), and Mn<sup>2+</sup> may also bind to the NADH dehydrogenase complex without altering electron transport in vivo (Gavin et al. 1992). To avoid cell death originating from NAD consumption or reduction, plants activate a mechanism to provide adequate NAD levels in cells, so NAD is re-synthesized when its level is reduced (Hashida et al. 2009). The two major pathways involved in the biosynthesis of NAD<sup>+</sup> from extracellular nicotinic acid or various intracellular NAD<sup>+</sup> decomposition products and tryptophan precursors are the de novo pathway or the salvage pathway, respectively (Sporty et al. 2009). These two pathways facilitate NAD biosynthesis for all organisms (Wang and Pichersky 2007). Some possible multistep routes were suggested from nicotinamide through nicotinic acid that culminate in NAD formation in the corresponding pyridine cycling pathway (Noctor et al. 2006). Thus, free nicotinamide is a primary by-product of the NAD cycle (Hashida et al. 2009) and is converted to nicotinic acid by nicotinamidase (Hunt et al. 2004). Either nicotinamide or nicotinic acid serves as a cellular NAD precursor; nicotinic acid generated 200- and 500-fold increased levels of NAD biosynthesis compared with nicotinamide or tryptophan, respectively, in the glia (Penberthy 2009). Berglund (1994) hypothesized that nicotinamide is a signal linking the antioxidative response of eukaryotic cells (Berglund 1994; Ohlsson et al. 2008), and nicotinamide is also predicted to serve as a cofactor for numerous enzymes. One of the most important activities of nicotinic acid is its role in photosynthetic processes in biological systems that occur via NADP (Hopkins 2006). Nicotinic acid is also a complexing agent for many metals, such as Mn, Co, Ni, Cu, and Zn (Suksrichavalit et al. 2009), and this property may support the mobility of divalent cations.

There is continuing interest in demonstrating the importance of metabolomics under different stress mechanisms in plants (Berglund and Ohlsson 1995; Kral'ova et al. 2012; Obata and Fernie 2012). To the best of our knowledge, elemental interactions in conjunction with metabolites have not been explored to date under conditions of Mn stress. Several works can be presented as examples of similar studies with perspectives distinct from this research. Baker et al. (2017) assessed occupational health using metabolomics under Mn stress conditions, whereas Ohlsson et al. (2008) studied increased metal (Cu, Zn, Cd) tolerance in *Salix* following nicotinamide and nicotinic acid exposure. The NAD salvage pathway, which diverges at nicotinamide (Wang and Pichersky 2007), or NAD biosynthesis, which plays important roles in plants even in the context of stress responses (Hashida et al.

2009; Hunt et al. 2004), was explored in detail. Additionally, the relationship between NAD and Mn was reported by Abbouni et al. (2004), Wang et al. (2014), and Bornhorst et al. (2012) in *Corynebacterium ammoniagenes*, cochlear organotypic cultures, and human cells, respectively. Moreover, from an elemental perspective, Mn transport, accumulation, and resistance mechanisms in plants (Millaleo et al. 2010) as well as the physiological response of *P. perfoliatum* to elevated manganese concentrations (Xue et al. 2018) serve as other recent examples even though these works were not directly related to the goal of this study.

Given these abovementioned connections and considering the proposed relationships between Mn and NAD, the objectives of this work were (1) to determine the effects of Mn on elemental uptake and transportation in *Verbascum olympicum* Boiss. and (2) to predict the role of the nicotinic acid/nicotinamide metabolites as possible chelating organic acids in the NAD pathway and in the mechanism to cope with oxidative stress in the presence of excess Mn. The important strategy in the first part of this study was to link excess manganese with the competitive and/or complementary effect of some elements. In the second part of this study, we sought to clarify the possible relationships between elements, in particular Mn with NAD, in plant metabolism. Finally, combining the effects that occur through metal mobility and NAD metabolites may allow to assess the survival capability of this species in more detail under Mn stress conditions. This combined, two-sided approach will therefore provide a starting point for the emerging field of metabolomics research in plant sciences by highlighting the importance of elemental perspectives beyond organic analysis.

## Materials and methods

### Plant cultivation and harvesting for analysis

Seeds of *Verbascum olympicum* Boiss. (Scrophulariaceae), which is one of the endemic species of Uludag Mountain (Bursa-Turkey), were collected from the alpine belt of Uludag (1850–1900 m) in August 2011. The potential of the species to restore the degraded ecosystems and its tolerance to many elements were revealed in earlier studies (Akpınar et al. 2015; Arslan et al. 2014; Guleryuz et al. 2006, 2015). Collected seeds were sterilized with 5% sodium hypochlorite for 5 min, rinsed with ultrapure water ( $18.3 \text{ M}\Omega \text{ cm}^{-1}$ , Zener Power I, Human Corp., Seoul, Korea) and grown in Hoagland's nutrient solution after germination. All the steps for germination and cultivation (Akpınar et al. 2015; Arslan et al. 2014) and the components of Hoagland's solution were previously reported (Hoagland and Arnon 1950; Xue et al. 2004). On the 10th day after germination, the seedlings were transferred to small plastic beakers ( $20 \times 15 \times 10 \text{ cm}$ ) filled

with 600 mL of one-tenth (v/v)-strength Hoagland's nutrient medium in a growth chamber (Heraeus Vötsch HPS500, Balingen, Germany). Plants were grown in a  $25 \text{ }^\circ\text{C}/15 \text{ }^\circ\text{C}$  day/night temperature regime with a 16-h light/8-h dark photoperiod and were illuminated by cool white fluorescent 36-W tubes that provided irradiance (400–700 nm) of approximately  $80 \mu\text{mol m}^{-2} \text{ s}^{-1}$ . The nutrient medium (pH 6.0) was renewed every 2 days, and its concentration was increased by 10% once a week. Eight-week-old seedlings (with 8 leaves) were exposed to three different concentrations of Mn supplied as  $\text{MnSO}_4$  (Merck, 105999, Darmstadt, Germany): 5 (control; CK), 50, and 200  $\mu\text{M}$  in 80% Hoagland's nutrient medium. Although 0 is evaluated as CK in our experiments and corresponds to cultivated plants without any additional Mn treatment in Hoagland's solution, the final Mn level of 5  $\mu\text{M}$  was specified for control samples because used Hoagland's solution contains approximately 5  $\mu\text{M}$  Mn. Four plant samples were harvested on days 1, 3, and 7 of the experiment and washed thoroughly with ultrapure water. Then, the plant components (roots and leaves) were separated. Two subsamples were used for elemental and organic analysis. One subsample of the roots and leaves was separately dried in an oven at  $105 \text{ }^\circ\text{C}$  for 24 h in clear paper bags. Dried samples were homogenized by grinding with a porcelain mortar and used for inductively coupled plasma–mass spectrometry (ICP-MS) analysis. The second subgroup of plant components was stored at  $-70 \text{ }^\circ\text{C}$  for nicotinic acid analysis by capillary electrophoresis (CE). Stress situations were assessed by determining hydrogen peroxide levels in one specimen that was harvested at CK and after the application of 50  $\mu\text{M}$  Mn (3rd day). Scanning electron microscopy with energy-dispersive X-ray spectroscopy (SEM-EDX) analyses were also performed with the same sample groups. GSH, glutathione disulfide (GSSG), and total phenolic content analyses were separately performed using CK and 200  $\mu\text{M}$  Mn-treated specimens (7th day).

### Trace element analysis

Mn, Fe, Zn, Cu, Mo, and B levels in the plant tissues were analyzed using an Elan 9000 ICP-MS (PerkinElmer SCIEX, Shelton, CT, USA) to assess the most abundant isotopes of the elements. The optimum instrumental conditions were as follows. The radio-frequency power was 1.0 kW, and the plasma and nebulizer argon flow rates were  $17.0 \text{ L min}^{-1}$  and  $0.85 \text{ L min}^{-1}$ , respectively. Samples were introduced at a flow rate of  $1.5 \text{ mL min}^{-1}$  with a dwell time of 50 ms (scanning mode: peak hopping; detector mode: dual). The classical open wet digestion with 3 mL  $\text{HNO}_3$  and 2 mL  $\text{H}_2\text{O}_2$  was applied in a borosilicate glass beaker. Although the biomass of each specimen may have varied, 0.01–0.03 g of samples was used for both roots and leaves. Digests were filtered through PVDF (polyvinylidene fluoride) syringe filters (0.45- $\mu\text{m}$  pore size, hydrophilic, Millex-HV, Millipore Corp., Bedford, MA,

USA) and diluted before analysis. External calibration curves were constructed with eight points ( $0.1\text{--}30\ \mu\text{g L}^{-1}$  for Mn) by diluting a multielement standard solution (Merck 110580). The instrumental limits of detection were calculated based on the standard deviation of the smallest quantitation level of the analyzed elements. The accuracy of the method was confirmed based on an analysis of certified reference materials (CRM), namely, GBW07605 tea leaves and NIST 1570 spinach leaves, that were purchased from the National Research Center for Certified Reference Materials (Beijing, China) and the National Institute of Standards and Technology (Gaithersburg, MD, USA), respectively. All validation parameters, quantification limits, and other instrumental parameters were previously reported (Guleryuz et al. 2015).

### Nicotinic acid analysis

The extraction of nicotinic acid was initiated by grinding the frozen plant components and separately weighing approximately 0.1 g of all samples. Alkaline hydrolysis using 15 mL of 1 M NaOH was performed for 45 min in an ultrasonic bath at 70 °C. An Elma LC-30H model ultrasonic bath (Singen, Germany) operated at an ultrasonic frequency of 35 kHz and a power of 240 W was used for this purpose. Samples were analyzed without dilution and filtered through 0.22- $\mu\text{m}$  hydrophilic polyvinylidene fluoride (PVDF) syringe filters (Millex-HV, Millipore) prior to analysis. All of the stock and sample solutions were stored at 4.0 °C until CE analysis. Beckman Coulter P/ACE MDQ capillary electrophoresis (Beckman Coulter, Inc. Fullerton, CA, USA) with a photo diode array detector and 32 Karat 8.0 software was used for the analysis. A bare fused-silica capillary column with a 75- $\mu\text{m}$  internal diameter and 375- $\mu\text{m}$  outside diameter (Beckman Coulter, PN 338454) with total and effective lengths of 70 cm and 50 cm, respectively, was used, and it was conditioned using methanol, 0.1 N HCl, 0.1 N NaOH (regenerator solution A, PN 338424), and run buffer A (PN 338426) according to the manufacturer's manual. Test mix B (PN 501333) was used to evaluate the performance of the column. The background electrolyte for separation was 25 mM dilute Tris buffer (PN 477427) (pH 4.7). The column was washed with electrolyte buffer for 5 min before and during all analyses. Samples and cartridges were stored at 25 °C, and the samples were injected at a pressure of 0.5 psi for 4 s. The separation voltage was + 30 kV. The UV absorption spectra were obtained from 190 to 300 nm with a detection wavelength of 254 nm.

### Hydrogen peroxide analysis

Fresh leaf and root samples were frozen for at least 24 h at  $-20\ ^\circ\text{C}$  in polyethylene centrifuge tubes and lyophilized at  $-45\ ^\circ\text{C}$  and 0.057 mBar using a Labconco FreeZone 1-L

lyophilizer (Kansas City, MO, USA). The  $\text{H}_2\text{O}_2$  determination assay was adapted from the method of Junglee et al. (2014). Lyophilized powder (100 mg) was homogenized with 2.5 mL of trichloroacetic acid (0.1% (w/v)), 5 mL of KI (1 M) and 2.5 mL of potassium phosphate buffer (10 mM, pH 7) at 4 °C for 10 min and centrifuged at 4000 rpm for 15 min at 4 °C. A Nuve/NF 800 model centrifuge (Ankara, Turkey) was used for separation purposes. Samples were incubated at room temperature ( $20\text{--}22\ ^\circ\text{C}$ ) for 20 min, and the supernatants were filtered through 0.45- $\mu\text{m}$  hydrophilic PVDF syringe filters. A calibration curve obtained with  $\text{H}_2\text{O}_2$  standard solutions (0 to 50 nmol) was prepared in 0.1% TCA with a total volume of 12.5 mL and used for quantification. All solutions contained 5 mL of KI and 2.5 mL of phosphate buffer. Then, the absorbance at 350 nm was recorded using a Shimadzu UV-1800 spectrophotometer (Shimadzu Corporation, Kyoto, Japan).

### Determination of total phenolic content

Briefly, 5 mL of methanol/water (80:20, v/v) were added to 1.5 g of lyophilized samples, which were then centrifuged at 3000 rpm for 10 min at room temperature ( $20\text{--}22\ ^\circ\text{C}$ ) in triplicate. Supernatants were collected and dried under nitrogen atmosphere, and the residue was dissolved in 4 mL of methanol/water (80:20, v/v). Total phenolic contents were determined using the modified Folin–Ciocalteu assay, which was adapted from Berker et al. (2013). Folin–Ciocalteu's reagent was diluted at a ratio of 1:4 with ultrapure water (1 volume Folin–Ciocalteu's phenol reagent + 3 volumes distilled water) prior to use. Lowry A solution was prepared from sodium carbonate (2.0% (w/v)) in 0.1 M NaOH solution, and Lowry B solution was prepared from copper (II) sulfate (0.5% (w/v)) in 1.0% sodium potassium tartrate ( $\text{NaKC}_4\text{H}_4\text{O}_6$ ) solution. Finally, Lowry C solution was prepared from Lowry A and Lowry B (50:1 (v/v)). In addition, 1.5 mL of  $\text{H}_2\text{O}$  was added to 0.5 mL of sample solution followed by 2.5 mL of Lowry C solution, and the mixture was allowed to stand for 10 min. Then, 0.25 mL of Folin reagent was added. Samples were stored for 20 min under dark conditions and centrifuged at 3000 rpm for 10 min at room temperature ( $20\text{--}22\ ^\circ\text{C}$ ). Calibration curves were constructed with six points (5 ppm to 50 ppm) for gallic acid. The absorbance was measured at 765 nm. The results are expressed in mg gallic acid/100 g of sample. All determinations were performed in triplicate.

### Determination of GSH and GSSG levels

GSH and its oxidized form, GSSG, were obtained from Sigma Chemicals (St. Louis MO, USA). Plant samples were prepared to determine GSH and GSSG levels based on the modified protocol published by Yilmaz et al. (2009). Briefly, 1 g of fresh plant samples (stored at  $-70\ ^\circ\text{C}$ ) was homogenized in

10 mL of Tris-EDTA buffer at pH 7.0 (Sigma chemicals), and 1 mL of homogenate was mixed with 1 mL of perchloric acid and centrifuged at 6000 rpm for 10 min at + 4 °C. Then, 1 mL of this solution was subjected to high-performance liquid chromatography (HPLC) analysis (Shimadzu, Kyoto Japan). The VP series HPLC included a pump (LC-10 ADVP), a diode array detector (SPD-10AVP), a column oven (CTO-10ASVP), an autosampler (SIL-10ADVP), and a degasser (DGU-14A), and Shimadzu Class VP software was used for analysis. Separation was performed with an analytical column (ODS 4, 150 × 4.6 mm i.d., 5 µm particle size). Working standard solutions of 0.05–0.5 ppm GSSG and 0.2–2 ppm GSH were used for calibration, and detection was performed at 210 nm. The column temperature was maintained at 40 °C, and the elution was performed with 50 mM NaClO<sub>4</sub> and 0.1% H<sub>3</sub>PO<sub>4</sub> at a flow rate of 1.0 mL min<sup>-1</sup>. The injection volume was 50 µL. All the injections were performed in triplicate.

### SEM-EDX analysis

The surface morphology and manganese residues on root surfaces were evaluated using a VEGA3 SB TESCAN scanning electron microscope (Czech Republic) that was fully integrated with a Bruker EasyEDX energy-dispersive X-ray microanalyzer. Lyophilized root samples were prepared by placing powder onto a conductive graphite strip after the samples were coated with gold. SEM images were recorded with an accelerating voltage of 20 kV.

### Statistical analysis

All statistical tests were performed at the significance level of 0.05 using SPSS 16.0 for Windows (SPSS Inc. 2007). The differences between the mean values of trace elements, the different Mn concentrations and the Mn exposure periods were analyzed by two-way ANOVA ( $n = 4$ ).

## Results and discussion

### Elemental analysis

Mn concentrations up to 500 mg kg<sup>-1</sup> are considered non-toxic, and Mn levels greater than 1500 mg kg<sup>-1</sup> are considered toxic to normal plants despite the fact that Mn is an essential trace element for plant growth (Xue et al. 2016; Xue et al. 2018). However, *V. olympicum* exhibited no visual Mn toxicity in response to treatment with 0–200 µmol L<sup>-1</sup> Mn in this study. Given the possible inhibitory effects of excess Mn on metabolic processes (Xue et al. 2016), it must be noted that the possibility of increased biomass but inhibited growth may occur as in *Chenopodium ambrosioides* L. under Mn stress (Xue et al. 2016). The major effect of Mn toxicity involves

inducing oxidative stress and a subsequent increase in reactive oxygen species (ROS) formation (Xue et al. 2016). H<sub>2</sub>O<sub>2</sub> is produced in plants during normal physiological processes and is also involved in oxidative cellular damage (Junglee et al. 2014), so we determined H<sub>2</sub>O<sub>2</sub> levels as an indicator of ROS formation to evaluate stress conditions. As the most stable form of ROS, intra- and intercellular H<sub>2</sub>O<sub>2</sub> levels increase during environmental stress (Slesak et al. 2007). H<sub>2</sub>O<sub>2</sub> levels were increased in leaves in contrast to that observed in roots. Nevertheless, selecting appropriate Mn treatment doses that are not too high to induce phytotoxicity or too low to induce stress may be important for understanding metabolic processes.

In addition to interfering with metabolic pathways, Mn inhibition is also indicated in the uptake and activity of some elements, such as Ca<sup>2+</sup>, Fe<sup>2+</sup>, and Mg<sup>2+</sup> (Xue et al. 2018), which may necessitate multielemental determination under excess Mn conditions to determine the complementary and competitive effects on elemental uptake in relevant metabolic processes. Tables 1 and 2 present the mean trace element levels and corresponding translocation factors (TF) in *V. olympicum* seedlings exposed to increasing Mn concentrations for 7 days. TF values reveal the transportation and distribution of metals in plant parts located below and above ground (Xue et al. 2018) and were calculated by dividing the content in the shoots by the content in the roots for each element ( $n = 4$ ) (Guleryuz et al. 2015). Mn levels were enhanced by Mn treatments (Table 1;  $P < 0.05$ ), and although increased Mn levels were observed for both roots and leaves, a difference was noted between plant parts in terms of the accumulation of this element. Given that all Mn treatments at each time point resulted in Mn concentrations greater than that noted in leaves (Table 1), the roots appear to be the main site of Mn accumulation in *V. olympicum*. Mn levels in these parts were up to 5680 ± 3300 mg kg<sup>-1</sup> dry weight (DW) in the 200 µM Mn-treated plants on the 7th day. This value exceeded the average threshold range of Mn levels in plant tissues (1–700 mg kg<sup>-1</sup> DW) (Visioli and Marmiroli 2013), demonstrating the Mn accumulation capacity of roots, so the possibility of the retention of excess Mn in this plant component in the form of insoluble Mn oxides was investigated. Sample morphology and Mn accumulation on the root surface were screened in SEM images, which are presented in Fig. 1 with detailed instrumental conditions provided under them. Results on selected points (from 1 to 5, on SEM images) represent the percentages of elemental distribution as weight (wt.%). When the elemental adsorption region was identified and further analyzed using an energy-dispersive X-ray spectrometer to assess elemental composition, Mn could be detected on the fine root regions of 200 µM Mn-treated roots after the 7th day. The elemental distribution results of the EDX analysis revealed that Mn and oxygen were the second and third, respectively, most accumulated elements on the surface. The major

**Table 1** Mn, Fe, and Zn contents (mg kg<sup>-1</sup> DW) in plant parts and TF values of the elements in *V. olympicum* seedlings exposed to different Mn treatment series and exposure periods (mean ± standard deviation; *n* = 4,  $\alpha$  = 0.05)

Treatments	Days	Roots	Leaves	TF
<b>Mn</b>				
5 $\mu$ M (CK)	1	506 ± 172	75.5 ± 18.1	0.16 ± 0.05
	3	1500 ± 390	65.3 ± 15.3	0.05 ± 0.03
	7	681 ± 180	86.4 ± 13.7	0.14 ± 0.06
50 $\mu$ M	1	1380 ± 380	79.3 ± 15.2	0.06 ± 0.02
	3	761 ± 324	76.4 ± 4.7	0.10 ± 0.09
	7	1370 ± 590	73.6 ± 15.0	0.06 ± 0.02
200 $\mu$ M	1	1110 ± 320	92.0 ± 20.1	0.09 ± 0.02
	3	3040 ± 1100	133 ± 28	0.05 ± 0.02
	7	5680 ± 3300	153 ± 13	0.04 ± 0.02
<b>Fe</b>				
5 $\mu$ M (CK)	1	4790 ± 2000	187 ± 31	0.05 ± 0.02
	3	5510 ± 2100	215 ± 68	0.04 ± 0.02
	7	1470 ± 420	199 ± 26	0.14 ± 0.04
50 $\mu$ M	1	9490 ± 5700	305 ± 109	0.05 ± 0.04
	3	9810 ± 4700	148 ± 18	0.02 ± 0.01
	7	6290 ± 1300	168 ± 35	0.03 ± 0.01
200 $\mu$ M	1	8400 ± 5700	186 ± 55	0.10 ± 0.10
	3	7260 ± 5200	168 ± 22	0.09 ± 0.09
	7	5240 ± 3700	196 ± 21	0.07 ± 0.07
<b>Zn</b>				
5 $\mu$ M (CK)	1	115 ± 5	47.3 ± 21.1	0.41 ± 0.19
	3	138 ± 4	49.0 ± 17.7	0.36 ± 0.13
	7	53.2 ± 18.1	41.5 ± 9.5	0.81 ± 0.15
50 $\mu$ M	1	165 ± 47	34.4 ± 11.7	0.23 ± 0.12
	3	156 ± 61	41.9 ± 4.6	0.32 ± 0.17
	7	137 ± 29	53.1 ± 10.3	0.40 ± 0.11
200 $\mu$ M	1	119 ± 42	45.7 ± 12.6	0.45 ± 0.25
	3	148 ± 33	32.9 ± 3.2	0.23 ± 0.04
	7	139 ± 49	49.3 ± 14.1	0.38 ± 0.12

Root Mn content,  $F_{\text{Concentration (2,69)}} = 13.95$ ,  $p = 0.00$ ,  $F_{\text{Duration (2,69)}} = 5.14$ ,  $p = 0.01$ ,  $F_{\text{Concentration} \times \text{Duration (4,69)}} = 5.19$ ,  $p = 0.00$ ; root Fe content,  $F_{\text{Concentration (2,69)}} = 4.31$ ,  $p = 0.02$ ,  $F_{\text{Duration (2,69)}} = 2.69$ ,  $p = 0.09$ ,  $F_{\text{Concentration} \times \text{Duration (4,69)}} = 0.09$ ,  $p = 0.99$ ; root Zn content,  $F_{\text{Concentration (2,69)}} = 5.62$ ,  $p = 0.01$ ,  $F_{\text{Duration (2,69)}} = 3.15$ ,  $p = 0.06$ ,  $F_{\text{Concentration} \times \text{Duration (4,69)}} = 1.85$ ,  $p = 0.15$ ; leaf Mn content,  $F_{\text{Concentration (2,69)}} = 35.80$ ,  $p = 0.00$ ,  $F_{\text{Duration (2,69)}} = 5.28$ ,  $p = 0.01$ ,  $F_{\text{Concentration} \times \text{Duration (4,69)}} = 5.17$ ,  $p = 0.00$ ; leaf Fe content,  $F_{\text{Concentration (2,69)}} = 0.65$ ,  $p = 0.53$ ,  $F_{\text{Duration (2,69)}} = 3.06$ ,  $p = 0.06$ ,  $F_{\text{Concentration} \times \text{Duration (4,69)}} = 4.34$ ,  $p = 0.001$ ; leaf Zn content,  $F_{\text{Concentration (2,69)}} = 0.23$ ,  $p = 0.80$ ,  $F_{\text{Duration (2,69)}} = 0.94$ ,  $p = 0.40$ ,  $F_{\text{Concentration} \times \text{Duration (4,69)}} = 1.69$ ,  $p = 0.18$

elements according to elemental distribution on point 5 were C, Mn, and O, with 32.2 wt.%, 24.1 wt.%, and 16.0 wt.%, respectively (Fig. 1). Therefore, it may be concluded that these accumulated residues were likely present in Mn-oxide forms, which are insoluble and adsorbed on the surface. Other studies

**Table 2** Cu, Mo, and B contents (mg kg<sup>-1</sup> DW) in plant parts and TF values of the elements in *V. olympicum* seedlings exposed to different Mn treatment series and exposure periods (mean ± standard deviation; *n* = 4,  $\alpha$  = 0.05)

Treatments	Days	Roots	Leaves	TF
<b>Cu</b>				
5 $\mu$ M (CK)	1	19.9 ± 4.5	9.5 ± 1.7	0.50 ± 0.13
	3	21.6 ± 10.6	13.0 ± 3.7	0.65 ± 0.12
	7	8.7 ± 2.0	9.8 ± 3.1	1.16 ± 0.37
50 $\mu$ M	1	22.1 ± 10.2	11.9 ± 4.2	0.57 ± 0.17
	3	24.7 ± 6.0	8.9 ± 1.1	0.39 ± 0.15
	7	24.6 ± 6.2	8.9 ± 3.2	0.38 ± 0.17
200 $\mu$ M	1	32.3 ± 10.5	10.2 ± 1.7	0.34 ± 0.14
	3	36.9 ± 16.6	8.6 ± 1.4	0.27 ± 0.12
	7	13.0 ± 3.9	15.2 ± 3.8	1.24 ± 0.51
<b>Mo</b>				
5 $\mu$ M (CK)	1	10.3 ± 2.7	2.6 ± 0.4	0.27 ± 0.09
	3	15.8 ± 2.8	2.1 ± 0.6	0.14 ± 0.05
	7	13.1 ± 1.1	2.9 ± 1.0	0.22 ± 0.06
50 $\mu$ M	1	24.2 ± 0.8	2.2 ± 0.3	0.09 ± 0.01
	3	25.0 ± 18.9	1.8 ± 0.1	0.10 ± 0.06
	7	16.0 ± 2.7	1.7 ± 0.1	0.11 ± 0.01
200 $\mu$ M	1	14.9 ± 2.1	3.0 ± 0.5	0.21 ± 0.06
	3	19.2 ± 4.5	2.5 ± 0.2	0.14 ± 0.03
	7	16.4 ± 7.6	2.9 ± 0.3	0.21 ± 0.10
<b>B</b>				
5 $\mu$ M (CK)	1	27.6 ± 3.2	72.7 ± 7.2	2.66 ± 0.39
	3	21.4 ± 6.9	73.1 ± 24.5	3.50 ± 1.08
	7	33.8 ± 14.7	83.9 ± 15.5	2.82 ± 1.13
50 $\mu$ M	1	55.0 ± 15.8	84.0 ± 22.0	1.58 ± 0.42
	3	28.6 ± 16.8	57.7 ± 11.0	2.72 ± 1.71
	7	24.0 ± 10.2	56.6 ± 14.3	2.75 ± 1.49
200 $\mu$ M	1	26.1 ± 9.8	82.2 ± 10.6	3.53 ± 1.38
	3	27.9 ± 6.0	78.7 ± 23.7	2.89 ± 0.88
	7	17.4 ± 9.7	84.1 ± 13.2	5.80 ± 2.63

Root Cu content,  $F_{\text{Concentration (2,69)}} = 4.43$ ,  $p = 0.02$ ,  $F_{\text{Duration (2,69)}} = 6.19$ ,  $p = 0.01$ ,  $F_{\text{Concentration} \times \text{Duration (4,69)}} = 2.22$ ,  $p = 0.09$ ; root Mo content,  $F_{\text{Concentration (2,69)}} = 4.42$ ,  $p = 0.02$ ,  $F_{\text{Duration (2,69)}} = 1.45$ ,  $p = 0.25$ ,  $F_{\text{Concentration} \times \text{Duration (4,69)}} = 0.72$ ,  $p = 0.58$ ; root B content,  $F_{\text{Concentration (2,69)}} = 3.64$ ,  $p = 0.04$ ,  $F_{\text{Duration (2,69)}} = 3.65$ ,  $p = 0.04$ ,  $F_{\text{Concentration} \times \text{Duration (4,69)}} = 3.71$ ,  $p = 0.02$ ; leaf Cu content,  $F_{\text{Concentration (2,69)}} = 0.77$ ,  $p = 0.47$ ,  $F_{\text{Duration (2,69)}} = 0.48$ ,  $p = 0.63$ ,  $F_{\text{Concentration} \times \text{Duration (4,69)}} = 4.23$ ,  $p = 0.01$ ; leaf Mo content,  $F_{\text{Concentration (2,69)}} = 11.37$ ,  $p = 0.00$ ,  $F_{\text{Duration (2,69)}} = 3.26$ ,  $p = 0.05$ ,  $F_{\text{Concentration} \times \text{Duration (4,69)}} = 1.07$ ,  $p = 0.39$ ; leaf B content,  $F_{\text{Concentration (2,69)}} = 2.66$ ,  $p = 0.09$ ,  $F_{\text{Duration (2,69)}} = 1.01$ ,  $p = 0.38$ ,  $F_{\text{Concentration} \times \text{Duration (4,69)}} = 1.53$ ,  $p = 0.22$

highlighted brown spots on the leaves of different plant species that were probably attributed to accumulation of Mn oxides (Xue et al. 2016). In contrast to these findings, this form of Mn was screened on the roots in this study and found to be consistent with the abovementioned Mn accumulation capacity of roots. In contrast to roots, the Mn accumulation capacity



**Fig. 1** Scanning electron microscopy images of root samples. **a** Mn-treated sample (7th day, 200 μM Mn). **b** Control sample (7th day, 5 μM Mn)

of the leaves of seedlings was not greater than the threshold range of Mn in plant tissues based on their mean Mn levels under all treatment conditions.

Manganese, which is taken up by epidermal root cells via an active transport system, can be adsorbed by negatively charged cell wall constituents of the apoplastic spaces of the root cell (Humphries et al. 2007) or transported as a divalent cation,  $Mn^{2+}$ , into the plants (Pittman 2005). Calculated TF values less than 1 indicate restricted translocation of Mn to the above-ground parts of this species (Table 1), and such low TF values can be attributed to species-specific Mn transport in *V. olympicum*. Xue et al. (2018) reported high TF values (> 1) in *Polygonum perforatum* plants exposed to Mn stress. Restricted Mn translocation also may be related to the formation of  $MnO_2$  in roots, and this form is not bioavailable in plants. The reduction in manganese may serve as a protective mechanism of *V. olympicum* against the negative effects of enhanced Mn in shoot cells. Inhibition of Mn translocation has also been reported in the literature as a mechanism of Mn tolerance in polish wheat plants, in which Mn also serves to enhance enzymatic activities, regulate non-enzymatic antioxidant levels, and control nutrient absorption and distribution (Sheng et al. 2015).

Element concentrations during plant growth in natural and controlled conditions and the interactions between the elements may affect the uptake and distribution of other elements (Arslan et al. 2014; Erdemir et al. 2017; Seven Erdemir 2017). Additionally, excessive levels of one nutrient may alter the behavior of others (Arslan et al. 2014; Guleryuz et al. 2015; Millaleo et al. 2010), possibly due to similarities between the chemical characteristics of the elements as previously described by Pittman (2005). Finally, nutrient interactions with

competitive or complementary behaviors should be taken into account, which is one of the aims of this study, but this strategy may be more important when attempting to understand natural growth conditions (Seven Erdemir 2017). In this context, the elements in Tables 1 and 2 were selected to observe the different translocation and/or accumulation characteristics of the other elements, beginning with roots that were exposed to excess Mn. According to Millaleo et al. (2010), excess Mn could alter the absorption, translocation, and utilization of other elements, such as Ca, Mg, Fe, and P, and based on the results of Shi et al. (2006), excess Mn was associated with reduced levels of Fe in the leaves of *Cucumis sativus* L. Excess Fe and Cd levels also inhibit  $Mn^{2+}$  accumulation. Moreover, the close ionic radii of  $Mn^{2+}$  and  $Fe^{2+}$ , which are between  $Ca^{2+}$  and  $Mg^{2+}$  levels, were previously mentioned (Pittman 2005). In general, all the described elemental levels, except Mn and Cu, were increased in the control samples compared with the levels noted in naturally spread *Verbascum olympicum* Boiss. from uncontaminated soils (Seven Erdemir 2017). When comparing the results with the naturally grown species, some parameters, such as the high concentration of concomitant metals and different pH values of soils of naturally grown species compared with those grown in hydroponic media (Xue et al. 2004), were not considered when drawing this conclusion regarding Cu as well as similar results noted for B, which will be explained below.

Comparing the effects of different dosage levels to the control group is the preferred method to explain any elemental interactions in hydroponics culture. Although the literature suggests that relationships with Ca, Fe, and Mg are generally noted with excess Mn treatments, the studied elements were selected depending on the constituents of Hoagland’s nutrient

medium, and the accuracy of the results was confirmed by CRM analysis as described in the experimental section. Thus, among these three suggested elements, only Fe is explained below based on the statistical evaluation. Interestingly, no significant correlation was observed ( $P > 0.05$ ) between the applied Mn dosage and Mg levels, and no further evaluation was proposed for Mg in this study.

According to metal uptake characteristics, plants can be classified as excluders, index plants, or accumulators (Wang et al. 2018a). Although some mechanisms, such as metal sequestration via organic compounds, subcellular compartmentalization, active metal efflux, and organic ligand exudation, are considered important, changes in growth under stress conditions could also indicate the protection capability of plants from metal toxicity (Wang et al. 2018a). Moreover, unaffected biomass production together with some physiological responses, i.e., promotion/inhibition of carbohydrate secretion and increased amino acid, peptide or protein production in different tissues and organs of hydroponically grown *Mirabilis jalapa* Linn. under Pb stress, were assessed by Fourier transform infrared spectrometry as indicators of Pb tolerance ability in the growth medium (Wang et al. 2018a). In this context, *V. olympicum* was determined to absorb higher levels of elements from Hoagland's solution and survive without any visual symptoms of toxicity under laboratory conditions (unpublished data). Given that the concentrations of the elements in all treatments were not below the reference levels reported earlier, these results suggest that manganese treatments generally do not result in any competition. For example, the mean Fe levels in the roots of 200  $\mu\text{M}$  Mn-treated seedlings on the 7th day ( $5240 \pm 3700 \text{ mg kg}^{-1} \text{ DW}$ ; Table 1) were considerably increased compared with the normal Fe levels in the plant ( $150 \text{ mg kg}^{-1} \text{ DW}$ ) (Markert 1996), which may be attributed to Fe accumulation in the roots due to the lack of competition between Fe and Mn for uptake. Although treatment with 50  $\mu\text{M}$  Mn increased Fe levels in the leaves on the first day (Table 1), Fe accumulation in the leaves was not observed at the end of the experimental period. This finding can be explained by the limited movement of Fe from the roots to above-ground portions of the plants, resulting in decreased Fe levels in the leaves. The TF values for Fe were also less than 1 (Table 1), which was also observed for Mn. Thus, the Fe transportation model in *V. olympicum* seedlings in the presence of increased Mn concentrations over the 7-day period was similar to the variation model for Mn.

Mn treatments also did not cause any inhibition of Zn uptake (Table 1). Although low TF values for Zn ( $< 1$ ) indicate a lack of Zn accumulation, the mean levels for all treatments and durations were not below the average range reported for plant tissues ( $15\text{--}150 \text{ mg kg}^{-1} \text{ DW}$ ; Markert 1996). Similar to Zn, the copper composition of *V. olympicum* seedlings was not negatively affected by the Mn treatments.

The mean Cu levels in all treatments ranged from 8.6 to  $15.2 \text{ mg kg}^{-1} \text{ DW}$  in the leaves and from 8.7 to  $36.9 \text{ mg kg}^{-1} \text{ DW}$  in the roots (Table 2). Considering the average range of Cu in plant tissues ( $2\text{--}20 \text{ mg kg}^{-1} \text{ DW}$  (Markert 1996)), the mean Cu levels in seedlings from all treatments did not reflect any alterations in Cu uptake and transportation in *V. olympicum* under conditions of excess Mn, and the mean TF value of 200  $\mu\text{M}$  Mn-treated seedlings on the 7th day ( $1.24 \pm 0.51$ ) also supports this conclusion. In contrast, Cu exhibits transportation capability in the context of a high dosage of Mn unlike most other elements that instead exhibit complementary effects and/or effects mimicking those of Cu and Mn. The major antioxidant defense system enzymes (SODs) require active catalytic metals (Cu or Mn) (Fukai and Ushio-Fukai 2011). In addition, SODs mimic the activity of copper complexes of nicotinic-carboxylic acids/pyridine derivatives, which are the targets of organic analysis in this study, highlighting their role in the antioxidant defense mechanism (Suksrichavalit et al. 2009). This information provides several reasons why copper transportation at high dosages helps plants to cope with stress.

It is also concluded that *V. olympicum* has the ability to take up Mo under manganese stress conditions based on Mo levels of  $1 \text{ mg kg}^{-1}$  or less in normal leaves, according to Kabata-Pendias (2011). Although the mean Mo contents in the leaves of this species varied from 1.7 to  $3.0 \text{ mg kg}^{-1} \text{ DW}$ , root Mo levels reached up to  $25.0 \pm 18.9 \text{ mg kg}^{-1} \text{ DW}$  with 50  $\mu\text{M}$  Mn treatment on the 3rd day (Table 2). Although the low TF values did not reveal any effective accumulation of Mo in the leaves, the mean leaf Mo levels indicate continued Mo metabolism in this species under Mn stress conditions. Thus, Mo levels are not affected by excess Mn application during plant growth, which may be explained by different routes and/or independent characteristics of these elements for plant metabolic processes. However, the results of two-way ANOVA suggest that there is still a relationship between Mn and Mo, as shown in Table 2.

High B concentrations were also measured in the leaves, indicating the B accumulation properties of this species even in conditions of excess manganese. High TF values, which were observed in seedlings exposed to 200  $\mu\text{M}$  Mn treatment ( $5.80 \pm 2.63$ ) on the 7th day, suggest that the increased Mn concentration in the environment has no detrimental effects on the B metabolism of *V. olympicum* (Table 2). Thus, among the assessed elements, only B exhibited extremely different characteristics under excess Mn, as its high transportation ability was demonstrated by its high TF values. A comparison of the measured B levels in leaves with the published range in naturally grown *V. olympicum* ( $22.8 \pm 10.7\text{--}40.2 \pm 7.7 \text{ mg kg}^{-1}$ ) (Seven Erdemir 2017) revealed that B levels increased to  $84.0 \text{ mg kg}^{-1}$  upon treatment with 50  $\mu\text{M}$  B and subsequently decreased to  $56.6 \text{ mg kg}^{-1}$  after 7 days. The behavior of B in conjunction with the organic analysis portion of this study is also detailed below.



Finally, in addition to the results of glasshouse experiments (Xue et al. 2018), it should be noted that element uptake by plants greatly depends on the soil fractions in which elements are distributed in their natural growing conditions. In this context, some significant findings related to understanding the effects of mineralogy and adsorption behavior in residues from mineral ore processing were taken into account by determining the exchangeable and total contents of some elements by inductively coupled plasma atomic emission spectroscopy as well as by evaluating the chemical characteristics of residues by X-ray powder diffraction patterns (Zhu et al. 2018) with regard to natural rehabilitation of bauxite residue disposal areas (Kong et al. 2018). Moreover, the pollution characteristics of surface runoff in manganese tailing wasteland was assessed by quantifying the six heavy metals (Cu, Ni, Pb, Zn, Mn, and Cr) in different ecological restoration areas; they were found to be strongly related to each other, mostly in an organic-bound state, while manganese was found to be in a less dissolved state in manganese tailing wasteland (Wang et al. 2018b). Although the migration behavior, transformation form, and leaching loss of heavy metals in natural ecosystems are also important depending on numerous environmental factors (Wang et al. 2018b) when there is co-exposure to two or more metals, antagonistic effects may come to the forefront by reducing the toxic effects of these pollutants on humans (Xue et al. 2017). Thus, apart from the effects of this kind of stress detailed here, elemental fractions and bound forms, which depend on internal or external factors, in the natural habitat of any plant are likely to be important for assessing the real environmental conditions influencing human exposure.

## Organic analysis

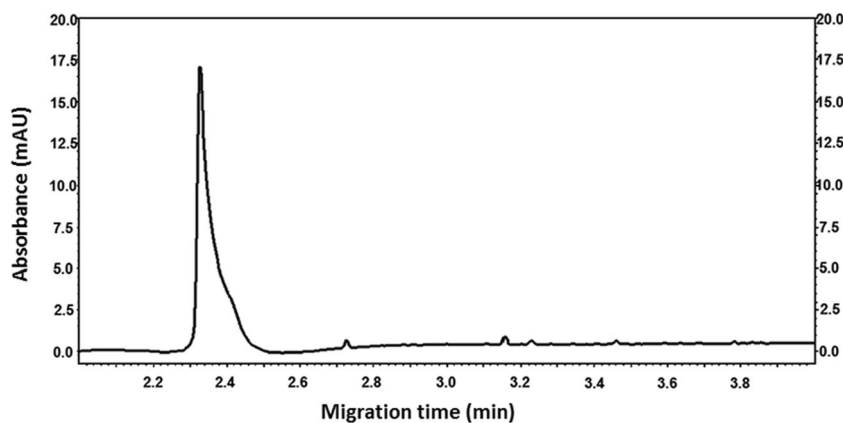
The terms niacin, nicotinamide, and vitamin B<sub>3</sub> are often used interchangeably. However, the strong alkaline hydrolysis conditions used here convert all nicotinamide or other forms to nicotinic acid (Lawrance 2005). Thus, the nicotinic acid levels presented hereafter refer to total nicotinic acid (nicotinic acid plus nicotinamide), which can be used as a summary parameter for the breakdown of the major products of NAD. Based on the data available from the literature explaining the properties of nicotinic acid in complex with metals and its interaction with NADP in photosynthesis, as detailed above, together with the interaction of Mn with organic acids to produce metabolically inactive compounds as one of the mechanism to reduce Mn stress (Xue et al. 2018), the following possibilities were examined: (i) the role of nicotinic acid/nicotinamide as a possible metal transporter for Mn, (ii) the use of nicotinic acid analysis to study its role as a metabolite in plant mechanisms under stress conditions to cope with excess Mn, and (iii) the possible presence of interactions between inorganic analysis

(manganese/other elements) and organic analysis (nicotinic acid) using samples exposed to Mn stress.

As an example of real sample analysis, the electropherogram of nicotinic acid in one root sample of *V. olympicum* (from the 7th day under 5  $\mu$ M manganese treatment) is presented in Fig. 2. Comparisons of the diode array detector spectra obtained by CE as well as the retention times of nicotinic acid standard solutions and real samples were used for identification. Importantly, depending on the sample preparation step (alkaline hydrolysis of nicotinic acid standards separately or together in a mixture with nicotinamide), little variation was noted in the retention times. Thus, all the samples had to be evaluated after application of the exact same conditions. Nicotinic acid levels in leaves and roots are presented in Table 3. In roots, nicotinic acid production was reduced followed by a slight increase in the 50  $\mu$ M Mn-treated plants on the 7th day. A significant correlation was observed ( $P = 0.00$ ) between the applied Mn dosage and nicotinic acid; however, no significant correlation was observed between the exposure duration and nicotinic acid levels ( $P > 0.05$ ) (Table 4). In leaves, a larger decrease was noted with time and increased Mn concentration ( $P = 0.01$ ,  $P = 0.00$ , and  $P = 0.02$  between nicotinic acid levels/Mn concentration, nicotinic acid levels/duration, and nicotinic acid levels/concentration  $\times$  duration, respectively) according to statistical analysis (Table 4).

Considering the increased Mn concentrations and dose-dependent significant decrease in the nicotinic acid levels in roots, increased element transportation capacity (especially of manganese) from roots to leaves could be expected due to the reduced nicotinic acid levels. This proposal depends on the fact that nicotinic acid has the ability to form complexes with various metals, as previously reported by Suksrichavalit et al. (2009). On the other hand, this expectation was not supported by the restricted translocation of the studied elements. Consequently, nicotinic acid does not appear to be a complexing agent or phytochelatin (which here refers to a complexing agent in plant chemistry and is used to describe the possible bidentate complexing property of nicotinic acid) for the transportation of elements in Mn-treated *V. olympicum* seedlings under controlled conditions. As indicated by their high TF values, only B and Cu (exclusively in 200  $\mu$ M Mn-treated samples) may complex with nicotinic acid for transportation based on the presented findings, but this hypothesis requires further assessment. This finding may also explain the reduced nicotinic acid levels in the roots. On the other hand, this mechanism could also lead to interrupted NAD formation from the salvage pathway through NAD degradation products, indicating the probable role of the de novo pathway. These pathways are summarized in Fig. S1 (supplementary material). If the NAD salvage pathway encountered a nicotinic acid catabolite, possible complex formation would be expected to affect the cycle based on elemental transportation as complexes. Among the other elements, the only one that

**Fig. 2** Electropherogram of nicotinic acid in one root sample of *V. olympicum* (7th day, 5  $\mu$ M manganese treatment)



behaves extremely differently in terms of the highest TF value against the highest Mn treatment was B (Table 2). Thus, decreased nicotinic acid levels could be an indicator of boron complexation and NAD degradation. The relationship between B and NAD under Mn stress is meaningful because Kabu and Akosman (2013) demonstrated that borate inhibits nicotinamide adenine dinucleotide, and the hydroxyl groups of NAD form complexes with the anionic form of B. B is actually a passively absorbed element and is transported into the root cells from the soil as  $H_3BO_3$  (Sun et al. 2013). This finding suggests that the uncharged form of B and the pH of the Hoagland's solution do not allow the complexed form of B to be transported. In this case, the transportation capability of B may reveal the essentiality of this element in cell wall systems (Seven Erdemir 2017). Furthermore, the affinity of B to NAD for complex formation was also mentioned by Reid et al. (2004), and it may interrupt the NAD cycle of NADPH conversion that produces GSH (Fig. S1, supplementary material).

GSH is an important non-enzymatic antioxidant that protects plants from oxidative stresses based on the increase in GSH levels in conditions with significantly reduced oxygen species (Cao et al. 2017). Given that Hameed et al. (2014) reported increased consumption of GSH for phytochelatin production upon Cd exposure, GSH synthesis ability is proposed to be crucial for metal protection via increased or

decreased plant tolerance depending on the levels of GSH, and the oxidized GSSG/GSH ratio is increased in *Silene cucubis* in response to Cu exposure. Thus, GSH is a parameter that is adaptive to metal stresses (Hameed et al. 2014). Nicotinic acid leads to the formation of NADPH and may enter the GSH cycle in the context of oxidative stress conditions caused by excess manganese, so an increase in the formation of NAD degradation products to form nicotinic acid and nicotinamide, as shown in Fig. S1 (supplementary material), may lead to the suppression of the NAD cycle, which produces GSH. In contrast, decreased levels of nicotinic acid in the roots may be an indicator of the active defense mechanism progressing through GSH in the presence of NADPH within different doses. As shown in Table 4, a significant correlation is noted between nicotinic acid and Mn treatment for both dosage and duration in leaves ( $P < 0.05$ ). Again, decreasing nicotinic acid levels may indicate that the properly functioning NAD cycle affects GSH at the molecular level.

Table 5 summarizes the results of the examined stress parameters, i.e., the hydrogen peroxide and total phenol levels as well as the GSH and GSSG contents in *V. olympicum*. Hydrogen peroxide levels were decreased in the roots ( $75.0 \pm 5.0$  nmol  $H_2O_2/g$  fresh weight) but increased in the leaves ( $1080 \pm 2$  nmol  $H_2O_2/g$  fresh weight) in response to Mn treatment compared with the control groups of the same samples ( $241 \pm 1$  nmol  $H_2O_2/g$  fresh weight and  $813 \pm 2$  nmol  $H_2O_2/g$

**Table 3** Total nicotinic acid levels ( $mg L^{-1}$ ) in leaves and roots of *V. olympicum* against Mn dosage and exposure duration

Mn treatments	Leaves			Roots		
	Treatment days					
	1	3	7	1	3	7
5 $\mu$ M (CK)	1.46 $\pm$ 0.11	1.15 $\pm$ 0.30	0.94 $\pm$ 0.09	1.43 $\pm$ 0.23	1.14 $\pm$ 0.32	1.11 $\pm$ 0.17
50 $\mu$ M	1.39 $\pm$ 0.24	1.02 $\pm$ 0.05	0.66 $\pm$ 0.11	1.18 $\pm$ 0.09	1.48 $\pm$ 0.02	1.25 $\pm$ 0.11
200 $\mu$ M	0.95 $\pm$ 0.07	1.19 $\pm$ 0.18	0.66 $\pm$ 0.10	0.96 $\pm$ 0.19	0.95 $\pm$ 0.05	1.02 $\pm$ 0.27

Result represents mean  $\pm$  standard deviation ( $n = 3$ )

**Table 4** Two-way ANOVA results for nicotinic acid levels in roots and leaves (all parameters were analyzed for Mn concentration × duration at the  $\alpha = 0.05$  significance level)

Source	Roots					Leaves				
	Type III sum of squares	df	Mean square	F	Sig.	Type III sum of squares	df	Mean square	F	Sig.
Corrected model	0.87 <sup>a</sup>	8	0.11	3.13	0.02	1.92 <sup>a</sup>	8	0.24	9.38	0.00
Intercept	36.9	1	36.9	1060	0.00	29.6	1	29.6	1150	0.00
Concentration	0.52	2	0.26	7.53	0.00	0.29	2	0.14	5.64	0.01
Duration	0.02	2	0.01	0.32	0.73	1.26	2	0.63	24.6	0.00
Concentration × duration	0.32	4	0.08	2.33	0.09	0.37	4	0.09	3.64	0.02
Error	0.63	18	0.04			0.46	18	0.03		
Total	38.4	27				31.9	27			
Corrected total	1.49	26				2.39	26			

<sup>a</sup> R squared = 0.81 (adjusted R squared = 0.72)

fresh weight in roots and leaves, respectively). On the other hand, total phenols exhibited a decreasing tendency in both roots and leaves with a large difference between the numerical values in leaves. GSH and GSSG levels were increased in the samples, and these findings support alteration of the ongoing NAD cycle, which may affect the GSH cycle. Qsaib et al. (2014) reported that increased hydrogen peroxide levels result in a significant decrease in the total amount of phenolic compounds under climatic changes and explained the interaction with the oxidation of phenolic compounds when H<sub>2</sub>O<sub>2</sub> levels are high. As a result, reduced total phenolic levels (Table 5) could be attributed to the survival capability of *V. olympicum* under Mn stress. A close relationship between B and the ascorbate/glutathione cycle was reported by Marschner (2012) based on reduced ascorbate/glutathione concentrations and B deficiency that were likely due to inhibition of ascorbate reductase and glutathione reductase. In roots, the trend of GSH reduction to less than detectable levels (Table 5) in the 200 μM Mn-treated sample is compatible with the decreased levels of B in roots (Table 2). This finding supports the proposed hypothesis in the literature and underscores the importance of B translocation. The relationships between B deficiency and chlorophyll decomposition as well as glucose and lignin synthesis-related genes (Liu et al. 2017) together with possible interactions between B and chlorophyll content have been previously explored (Hajiboland et al. 2014; Oosterhuis and Zhao 2001). According to Marschner (2012), B deficiency influences photosynthesis and possibly originates from lipid oxidation of the thylakoidal membranes, resulting in a reduced quantum yield and a less efficient Photosystem II (PS II). Therefore, a possible link could be expected between B and Mn in photosynthesis.

It must be considered that the Hoagland’s solution used for seedling cultivation might produce colloidal manganese structures that may cause co-precipitation of many elements

in the growing medium depending on the pH conditions (pH 6.0). Thus, any manganese oxide form may lead to the enrichment of the studied elements onto the colloidal structures of manganese, which may cover the root surfaces. The adsorption characteristics of manganese dioxide for Cu, Ni, Zn, Cd, and Pb were reported by Pretorius and Linder (2001) based on thermodynamic data analysis to predict the transport of metals in natural systems. Separation of trace metals via the manganese dioxide collection method was also introduced by Reynolds and Tyler (1964) for analytical application depending on the co-precipitation of the mixtures. Moreover, the colloid-chemical properties of manganese dioxide were studied at neutral and alkaline pH values by Morgan and Stumm (Morgan and Stumm 1964). The oxidation kinetics of L-tryptophan, which is the precursor of the de novo pathway of the NAD cycle by water-soluble and colloidal MnO<sub>2</sub> in aqueous-acidic medium was reported by Kabir-ud-Din et al. (2008), whereas colloidal MnO<sub>2</sub> sols are negatively charged in aqueous solutions. Thus, manganese precipitation as MnO<sub>2</sub> seems possible under the high manganese application conditions of the Hoagland’s solution and may adsorb divalent cations, prevent transportation to leaves, and complex with L-tryptophan to disturb the de novo pathway of NAD. Considering this possibility, decreased nicotinic acid levels may only be associated with the progression of the salvage pathway to GSH through the conversion of degradation products to cope with stress in the roots of plants. Although plants can develop or maintain stress metabolism through GSH for Mn tolerance to cope with oxidative stress, it is important to consider that Mn may also be utilized and consumed to stimulate the activity of nicotinamidase, which can be used for overall NAD production in the salvage pathway from degraded nicotinamide to form nicotinic acid as detailed in the literature data above.

**Table 5** Summary of stress parameters under Mn exposure

Treatment series	GSH (mg kg <sup>-1</sup> )		GSSG (mg kg <sup>-1</sup> )	
	5 μM (CK)	200 μM Mn, 7th day	5 μM (CK)	200 μM Mn, 7th day
Root	82.2 ± 9.2	58.4 ± 4.0	< LOQ <sup>a</sup>	1.20 ± 0.10
Leaf	48.4 ± 5.8	57.4 ± 7.2	81.6 ± 9.2	113.2 ± 12.8
Limits of detection	0.3 mg kg <sup>-1</sup>		0.4 mg kg <sup>-1</sup>	
Limits of quantitation	0.7 mg kg <sup>-1</sup>		1.0 mg kg <sup>-1</sup>	
Treatment series	Total phenol (mg gallic acid/100 g)		H <sub>2</sub> O <sub>2</sub> (nmol H <sub>2</sub> O <sub>2</sub> /g fresh weight)	
	5 μM (CK)	200 μM Mn, 7th day	5 μM (CK)	50 μM Mn, 3rd day
Root	3530 ± 32	3200 ± 1	241 ± 1	75.0 ± 5.0
Leaf	5320 ± 1	4840 ± 29	813 ± 2	1080 ± 2

<sup>a</sup> Under quantitation limit

## Conclusions

Given that mutual, antagonistic, or synergistic interactions among elements with bio-ligands may affect their uptake by plants, the influence of elements on the nutritional balance of *V. olympicum* was evaluated. Under the applied dosages and duration of this study, this species exhibits a survival mechanism to cope with oxidative stress originating from manganese. We conclude that *V. olympicum* is capable of accumulating high concentrations of Mn in its roots under artificial excess Mn conditions. The translocation properties of some trace elements were unaffected by Mn, whereas B was affected. However, the phytochelatin capability of nicotinic acid could not be assessed for element transportation due to the small TF values. Selected trace elements were limited based on Hoagland's nutrient composition and accuracy studies and were measured under excess Mn treatments, which cause stress conditions but not phytotoxicity to *V. olympicum*. Variations in and the statistical relationships among elements during the applied Mn dosage and duration were used to evaluate the responses of *V. olympicum* and understand the possible interactions between NAD and the oxidative stress pathways selecting nicotinic acid as an organic acid, which is also a decomposition product of NAD. Decreased levels of nicotinic acid in roots and leaves indicate the turnover of NAD from the salvage pathway. Finally, a small reduction in nicotinic acid levels may be a mechanism to cope with stress derived from excess Mn and facilitate proper progression of oxidative stress metabolism in this species.

The proposed analytical approach, which was combined with elemental and organic analysis techniques, may yield further studies on a range of topics, including metal mobility in soil and plant species. This perspective could also expand the importance of vitamin and metal interactions, given that Mn and nicotinic acid are components of vitamin B. There is still much to learn about the unknown mechanisms of elements in this area of research, and the results obtained in this study provide preliminary knowledge to understand the pathway involved in manganese transportation in metabolomic networks of NAD formation via enzyme responses and under stress conditions.

**Acknowledgments** Seed collection was performed with the permission of the General Directorate of Nature Protection and National Parks of the Republic of Turkey Ministry of Forestry and Water Affairs. The authors would like to thank Aysegul Akpinar and Ozge Gungor for their help with the seedlings/plant cultivation. The Commission of Scientific Research Projects of Uludag University (project number F-2008/25) is also gratefully acknowledged for providing inductively coupled plasma–mass spectrometry and capillary electrophoresis equipment. Parts of this study were presented as posters at the 14th International Conference on Environmental Science and Technology (CEST2015) in Greece and the 7th National Analytical Chemistry Congress in Turkey. The authors thank the Scientific and Technological Research Council of Turkey/Bursa Test and Analysis Laboratory (TUBITAK-BUTAL) for their technical support for SEM-EDX analysis as well as hydrogen peroxide and total phenolic assessments.

**Funding information** This work was supported by the Commission of Scientific Research Projects of Uludag University under grant number KUAP(F)-2014/20 (to U.S. Erdemir).

## Compliance with ethical standards

**Conflict of interest** The authors declare that they have no conflict of interest.

**Ethical statement** This article does not contain any studies with human participants or animals.

## References

- Abbouni B, Elhariry HM, Auling G (2004) Overproduction of NAD(+) and 5'-inosine monophosphate in the presence of 10 μM Mn<sup>2+</sup> by a mutant of *Corynebacterium ammoniagenes* with thermosensitive nucleotide reduction (nrd(ts)) after temperature shift. Arch Microbiol 182(2–3):119–125. <https://doi.org/10.1007/s00203-004-0674-4>
- Akpinar A, Arslan H, Guleryuz G, Kirmizi S, Erdemir US, Gucer S (2015) Ni-induced changes in nitrate assimilation and antioxidant metabolism of *Verbascum olympicum* Boiss.: could the plant be useful for phytoremediation or/and restoration purposes? Int J Phytoremediation 17(6):546–555. <https://doi.org/10.1080/15226514.2014.922926>
- Arslan H, Guleryuz G, Akpinar A, Kirmizi S, Erdemir US, Gucer S (2014) Responses of ruderal *Verbascum olympicum* Boiss.

- (Scrophulariaceae) growing under cadmium stress. *Clean-Soil Air Water* 42(6):824–835. <https://doi.org/10.1002/clen.201300219>
- Baker MG, Simpson CD, Lin YS, Shireman LM, Seixas N (2017) The use of metabolomics to identify biological signatures of manganese exposure. *Ann Work Expo Health* 61(4):406–415. <https://doi.org/10.1093/annweh/wxx032>
- Berglund T, Ohlsson AB (1995) Defensive and secondary metabolism in plant tissue cultures, with special reference to nicotinamide, glutathione and oxidative stress. *Plant Cell Tissue Organ Cult* 43(2):137–145. <https://doi.org/10.1007/BF00052169>
- Berglund T (1994) Nicotinamide, a missing link in the early stress-response in eukaryotic cells—a hypothesis with special reference to oxidative stress in plants. *FEBS Lett* 351(2):145–149. [https://doi.org/10.1016/0014-5793\(94\)00850-7](https://doi.org/10.1016/0014-5793(94)00850-7)
- Berker KI, Olgun FAO, Ozyurt D, Demirata B, Apak R (2013) Modified Folin-Ciocalteu antioxidant capacity assay for measuring lipophilic antioxidants. *J Agric Food Chem* 61(20):4783–4791. <https://doi.org/10.1021/jf400249k>
- Bornhorst J, Ebert F, Lohren H, Humpf HU, Karst U, Schwerdtle T (2012) Effects of manganese and arsenic species on the level of energy related nucleotides in human cells. *Metallomics* 4(3):297–306. <https://doi.org/10.1039/c2mt00164k>
- Cao YN, Ma CX, Chen GC, Zhang JF, Xing BS (2017) Physiological and biochemical responses of *Salix integra* Thunb. under copper stress as affected by soil flooding. *Environ Pollut* 225:644–653. <https://doi.org/10.1016/j.envpol.2017.03.040>
- Demirevska-Kepova K, Simova-Stoilova L, Stoyanova Z, Holzer R, Feller U (2004) Biochemical changes in barley plants after excessive supply of copper and manganese. *Environ Exp Bot* 52(3):253–266. <https://doi.org/10.1016/j.envexpbot.2004.02.004>
- de Varennes A, Carneiro JP, Goss MJ (2001) Characterization of manganese toxicity in two species of annual medics. *J Plant Nutr* 24(12):1947–1955. <https://doi.org/10.1081/PLN-100107606>
- Erdemir US, Arslan H, Guleryuz G, Gucer S (2017) Elemental composition of plant species from an abandoned tungsten mining area: are they useful for biogeochemical exploration and/or phytoremediation purposes? *Bull Environ Contam Toxicol* 98(3):299–303. <https://doi.org/10.1007/s00128-016-1899-z>
- Foyer CH, Noctor G (2011) Ascorbate and glutathione: the heart of the redox hub. *Plant Physiol* 155(1):2–18. <https://doi.org/10.1104/pp.110.167569>
- Fukai T, Ushio-Fukai M (2011) Superoxide dismutases: role in redox signaling, vascular function, and diseases. *Antioxid Redox Signal* 15(6):1583–1606. <https://doi.org/10.1089/ars.2011.3999>
- Gavin CE, Gunter KK, Gunter TE (1992) Mn<sup>2+</sup> sequestration by mitochondria and inhibition of oxidative-phosphorylation. *Toxicol Appl Pharmacol* 115(1):1–5. [https://doi.org/10.1016/0041-008X\(92\)90360-5](https://doi.org/10.1016/0041-008X(92)90360-5)
- Guleryuz G, Arslan H, Izgi B, Gucer S (2006) Element content (Cu, Fe, Mn, Ni, Pb, and Zn) of the ruderal plant *Verbascum olympicum* Boiss. from East Mediterranean. *Z Naturforsch C* 61(5–6):357–362. <https://doi.org/10.1515/znc-2006-5-610>
- Guleryuz G, Erdemir US, Arslan H, Akpinar A, Cicek A, Gucer S (2015) Variation in trace element mobility and nitrogen metabolism of *Verbascum olympicum* Boiss. under copper stress. *Chem Ecol* 31(6):494–509. <https://doi.org/10.1080/02757540.2015.1043285>
- Hajiboland R, Bahrami-Rad S, Bastani S (2014) Aluminum alleviates boron-deficiency induced growth impairment in tea plants. *Biol Plant* 58(4):717–724. <https://doi.org/10.1007/s10535-014-0425-6>
- Hameed A, Sharma I, Kumar A, Azooz MM, Lone HA, Ahmad P (2014) Glutathione metabolism in plants under environmental stress. In: Ahmad P (ed) Oxadative damage to plants: antioxidant networks and signaling. Academic Press, USA, pp 183–200. <https://doi.org/10.1016/B978-0-12-799963-0.00006-X>
- Hashida SN, Takahashi H, Uchimiya H (2009) The role of NAD biosynthesis in plant development and stress responses. *Ann Bot* 103(6):819–824. <https://doi.org/10.1093/aob/mcp019>
- Hoagland DR, Aron DI (1950) The water-culture method for growing plants without soil. California Agric. Exp. Station, Circular No.347, California, USA, pp 1–32
- Hopkins WG (2006) Photosynthesis and respiration. Infobase Publishing, New York
- Humphries J, Stangoulis J, Graham R (2007) Manganese. In: Barker A, Pilbeam D (eds) Handbook of plant nutrition. Taylor & Francis, Florida, USA, pp 351–366
- Hunt L, Lerner F, Ziegler M (2004) NAD-new roles in signalling and gene regulation in plants. *New Phytol* 163(1):31–44. <https://doi.org/10.1111/j.1469-8137.2004.01087.x>
- Jackson JF, Atkinson MR (1966) The requirement for bivalent cations in formation of nicotinamide-adenine dinucleotide by nicotinamide mononucleotide adenylyltransferase of pig-liver nuclei. *Biochem J* 101(1):208–213
- Junglee S, Urban L, Sallanon H, Lopez-Lauri F (2014) Optimized assay for hydrogen peroxide determination in plant tissue using potassium iodide. *Am J Analyt Chem* 5:730–736. <https://doi.org/10.4236/ajac.2014.511081>
- Kabata-Pendias A (2011) Trace elements in soils and plants. CRC Press, Boca Raton
- Kabir-ud-Din, Altaf M, Akram M (2008) The kinetics of oxidation of L-tryptophan by water-soluble colloidal manganese dioxide. *J Dispers Sci Technol* 29(6):809–816. <https://doi.org/10.1080/01932690701781410>
- Kabu M, Akosman MS (2013) Biological effects of boron. In: Whitacre DM (ed) Reviews of environmental contamination and toxicology, vol 225. Springer, New York, pp 57–75. [https://doi.org/10.1007/978-1-4614-6470-9\\_2](https://doi.org/10.1007/978-1-4614-6470-9_2)
- Katoh A, Uenohara K, Akita M, Hashimoto T (2006) Early steps in the biosynthesis of NAD in Arabidopsis start with aspartate and occur in the plastid. *Plant Physiol* 141(3):851–857. <https://doi.org/10.1104/pp.106.081091>
- Kral'ova K, Jampilek J, Ostrovsky I (2012) Metabolomics-useful tool for study of plant responses to abiotic stresses. *Ecol Chem Eng S* 19(2):133–161. <https://doi.org/10.2478/v10216-011-0012-0>
- Kramer U (2010) Metal hyperaccumulation in plants. In: Annual review of plant biology, vol 61 Merchant S, Briggs WR, Ort D (eds). *Ann Rev Plant Biol* 61:517–534. <https://doi.org/10.1146/annurev-arplant-042809-112156> Annual Reviews, USA
- Kong XF, Tian T, Xue SG, Hartley W, Huang LB, Wu C, Li CX (2018) Development of alkaline electrochemical characteristics demonstrates soil formation in bauxite residue undergoing natural rehabilitation. *Land Degrad Dev* 29(1):58–67. <https://doi.org/10.1002/ldr.2836>
- Lawrance P (2005) Niacin (vitamin B<sub>3</sub>)—a review of analytical methods for use in food. Government Chemist Programme Report., Report no. LGC/R/2014/385, LGC Limited, Teddington, UK
- Liu X, Zhang JW, Guo LX, Liu YZ, Jin LF, Hussain SB, Du W, Deng Z, Peng SA (2017) Transcriptome changes associated with boron deficiency in leaves of two citrus scion-rootstock combinations. *Front Plant Sci* 8: Article Number: 317. <https://doi.org/10.3389/fpls.2017.00317>
- Macfie SM, Taylor GJ (1992) The effects of excess manganese on photosynthetic rate and concentration of chlorophyll in *Triticum aestivum* grown in solution culture. *Physiol Plant* 85(3):467–475. <https://doi.org/10.1034/j.1399-3054.1992.850309.x>
- Markert B (1996) Instrumental element and multi-element analysis of plant samples: methods and applications. John Wiley & Sons, Chichester, New York
- Marschner H (1995) Mineral nutrition of higher plants. Academic Press, London

- Marschner H (2012) Mineral nutrition of higher plants, 3rd edn. Academic Press, London
- Martinez M, Bernal P, Almela C, Velez D, Garcia-Agustin P, Serrano R, Navarro-Avino J (2006) An engineered plant that accumulates higher levels of heavy metals than *Thlaspi caerulescens*, with yields of 100 times more biomass in mine soils. *Chemosphere* 64(3):478–485. <https://doi.org/10.1016/j.chemosphere.2005.10.044>
- Millaleo R, Reyes-Diaz M, Ivanov AG, Mora ML, Alberdi M (2010) Manganese as essential and toxic element for plants: transport, accumulation and resistance mechanisms. *J Soil Sci Plant Nutr* 10(4): 476–494. <https://doi.org/10.4067/S0718-95162010000200008>
- Morgan JJ, Stumm W (1964) Colloid-chemical properties of manganese dioxide. *J Colloid Sci* 19(4):347–359
- Noctor G, Queval G, Gakiere B (2006) NAD(P) synthesis and pyridine nucleotide cycling in plants and their potential importance in stress conditions. *J Exp Bot* 57(8):1603–1620. <https://doi.org/10.1093/jxb/erj202>
- Obata T, Fernie AR (2012) The use of metabolomics to dissect plant responses to abiotic stresses. *Cell Mol Life Sci* 69(19):3225–3243. <https://doi.org/10.1007/s00018-012-1091-5>
- Ohlsson AB, Landberg T, Berglund T, Greger M (2008) Increased metal tolerance in *Salix* by nicotinamide and nicotinic acid. *Plant Physiol Biochem* 46(7):655–664. <https://doi.org/10.1016/j.plaphy.2008.04.004>
- Oosterhuis DM, Zhao D (2001) Effect of boron deficiency on the growth and carbohydrate metabolism of cotton. In: Horst W.J. et al. (Eds.) *Plant nutrition. Developments in plant and soil sciences*, vol 92. pp 166–167, Springer, Dordrecht. [https://doi.org/10.1007/0-306-47624-X\\_80](https://doi.org/10.1007/0-306-47624-X_80)
- Penberthy WT (2009) Nicotinic acid-mediated activation of both membrane and nuclear receptors towards therapeutic glucocorticoid mimetics for treating multiple sclerosis. *PPAR Res* Article Number: 853707. <https://doi.org/10.1155/2009/853707>
- Petolino JF, Collins GB (1985) Manganese toxicity in tobacco (*Nicotiana tabacum* L.) callus and seedlings. *J Plant Physiol* 118(2):139–144. [https://doi.org/10.1016/S0176-1617\(85\)80142-5](https://doi.org/10.1016/S0176-1617(85)80142-5)
- Pittman JK (2005) Managing the manganese: molecular mechanisms of manganese transport and homeostasis. *New Phytol* 167(3):733–742. <https://doi.org/10.1111/j.1469-8137.2005.01453.x>
- Pretorius PJ, Linder PW (2001) The adsorption characteristics of delta-manganese dioxide: a collection of diffuse double layer constants for the adsorption of H<sup>+</sup>, Cu<sup>2+</sup>, Ni<sup>2+</sup>, Zn<sup>2+</sup>, Cd<sup>2+</sup> and Pb<sup>2+</sup>. *Appl Geochem* 16(9–10):1067–1082. [https://doi.org/10.1016/S0883-2927\(01\)00011-7](https://doi.org/10.1016/S0883-2927(01)00011-7)
- Qsaib S, Ikbal FEZ, Faize M, Koussa T (2014) Changes in levels of hydrogen peroxide and phenolic compounds in grapevine latent buds during the annual cycle. *International Journal of Scientific and Research Publications (IJSRP)*, Volume 4, Issue 5, May 2014 Edition
- Rahman A, Nahar K, Hasanuzzaman M, Fujita M (2016) Manganese-induced cadmium stress tolerance in rice seedlings: coordinated action of antioxidant defense, glyoxalase system and nutrient homeostasis. *C R Biol* 339(11–12):462–474. <https://doi.org/10.1016/j.crv.2016.08.002>
- Reid RJ, Hayes JE, Post A, Stangoulis JCR, Graham RD (2004) A critical analysis of the causes of boron toxicity in plants. *Plant Cell Environ* 27(11):1405–1414. <https://doi.org/10.1111/j.1365-3040.2004.01243.x>
- Reynolds GF, Tyler FS (1964) Studies of the separation of trace metals by the manganese dioxide “collection” method. Part II. The behaviour of lead: determination of antimony and tin in the presence of lead. *Analyst* 89:579–586. <https://doi.org/10.1039/AN9648900579>
- Seven Erdemir U (2017) Boron and molybdenum contents of *Verbascum olympicum* Boiss. growing around an abandoned tungsten mine: a case study for ecological problem solving. *J Turkish Chem Soc Sect A: Chem-JOTCSA* 4(2):489–500. <https://doi.org/10.18596/jotcsa.282219>
- Sheng HJ, Zeng J, Yan F, Wang XL, Wang Y, Kang HY, Fan X, Sha LN, Zhang HQ, Zhou YH (2015) Effect of exogenous salicylic acid on manganese toxicity, mineral nutrients translocation and antioxidative system in polish wheat (*Triticum polonicum* L.). *Acta Physiol Plant* 37(2): Article Number: UNSP 32. <https://doi.org/10.1007/s11738-015-1783-1>
- Shi QH, Bao ZY, Zhu ZJ, He Y, Qian QQ, Yu JQ (2005) Silicon mediated alleviation of Mn toxicity in *Cucumis sativus* in relation to activities of superoxide dismutase and ascorbate peroxidase. *Phytochemistry* 66(13):1551–1559. <https://doi.org/10.1016/j.phytochem.2005.05.006>
- Shi QH, Zhu ZJ, Xu M, Qian QQ, Yu JQ (2006) Effect of excess manganese on the antioxidant system in *Cucumis sativus* L. under two light intensities. *Environ Exp Bot* 58(1–3):197–205. <https://doi.org/10.1016/j.envexpbot.2005.08.005>
- Slesak I, Libik M, Karpinska B, Karpinski S, Miszalski Z (2007) The role of hydrogen peroxide in regulation of plant metabolism and cellular signalling in response to environmental stresses. *Acta Biochim Pol* 54(1):39–50
- Smith AM, Coupland G, Dolan L, Harberd N, Jones J, Martin C, Sablowski R, Amey A (2010) *Plant biology*. Garland Science, Taylor and Francis Group, LLC, New York
- Sporty J, Lin SJ, Kato M, Ognibene T, Stewart B, Turteltaub K, Bench G (2009) Quantitation of NAD(+) biosynthesis from the salvage pathway in *Saccharomyces cerevisiae*. *Yeast* 26(7):363–369. <https://doi.org/10.1002/yea.1671>
- Suksrichavalit T, Prachayasittikul S, Nantasenam C, Isarakura-Na-Ayudhya C, Prachayasittikul V (2009) Copper complexes of pyridine derivatives with superoxide scavenging and antimicrobial activities. *Eur J Med Chem* 44(8):3259–3265. <https://doi.org/10.1016/j.ejmech.2009.03.033>
- Sun T, Wang YP, Wang ZY, Liu P, Xu GD (2013) The effects of molybdenum and boron on the rhizosphere microorganisms and soil enzyme activities of soybean. *Acta Physiol Plant* 35(3):763–770. <https://doi.org/10.1007/s11738-012-1116-6>
- Sytar O, Kumar A, Latowski D, Kuczynska P, Strzalka K, Prasad MNV (2013) Heavy metal-induced oxidative damage, defense reactions, and detoxification mechanisms in plants. *Acta Physiol Plant* 35(4): 985–999. <https://doi.org/10.1007/s11738-012-1169-6>
- Visioli G, Marmiroli N (2013) The proteomics of heavy metal hyperaccumulation by plants. *J Proteome* 79:133–145. <https://doi.org/10.1016/j.jprot.2012.12.006>
- Wang GD, Pichersky E (2007) Nicotinamidase participates in the salvage pathway of NAD biosynthesis in *Arabidopsis*. *Plant J* 49(6):1020–1029. <https://doi.org/10.1111/j.1365-313X.2006.03013.x>
- Wang L, Ding DL, Salvi R, Roth JA (2014) Nicotinamide adenine dinucleotide prevents neuroaxonal degeneration induced by manganese in cochlear organotypic cultures. *Neurotoxicology* 40:65–74. <https://doi.org/10.1016/j.neuro.2013.11.007>
- Wang J, Ye S, Xue SG, Hartley W, Wu H, Shi LZ (2018a) The physiological response of *Mirabilis jalapa* Linn. to lead stress and accumulation. *Int Biodeterior Biodegradation* 128:11–14. <https://doi.org/10.1016/j.ibiod.2016.04.030>
- Wang J, Cheng QY, Xue SG, Rajendran M, Wu C, Liao JX (2018b) Pollution characteristics of surface runoff under different restoration types in manganese tailing wasteland. *Environ Sci Pollut Res* 25(10):9998–10005. <https://doi.org/10.1007/s11356-018-1338-2>
- Xue SG, Chen YX, Reeves RD, Baker AJM, Lin Q, Fernando DR (2004) Manganese uptake and accumulation by the hyperaccumulator plant *Phytolacca acinosa* Roxb. (Phytolaccaceae). *Environ Pollut* 131(3): 393–399. <https://doi.org/10.1016/j.envpol.2004.03.011>
- Xue SG, Zhu F, Wu C, Lei J, Hartley W, Pan WS (2016) Effects of manganese on the microstructures of *Chenopodium ambrosioides*

- L., a manganese tolerant plant. *Int J Phytoremediation* 18(7):710–719. <https://doi.org/10.1080/15226514.2015.1131233>
- Xue SG, Shi LZ, Wu C, Wu H, Qin YY, Pan WS, Hartley W, Cui MQ (2017) Cadmium, lead, and arsenic contamination in paddy soils of a mining area and their exposure effects on human HEPG2 and keratinocyte cell-lines. *Environ Res* 156:23–30. <https://doi.org/10.1016/j.envres.2017.03.014>
- Xue SG, Wang J, Wu C, Li S, Hartley W, Wu H, Zhu F, Cui MQ (2018) Physiological response of *Polygonum perfoliatum* L. following exposure to elevated manganese concentrations. *Environ Sci Pollut Res* 25(1):132–140. <https://doi.org/10.1007/s11356-016-8312-7>
- Yilmaz O, Keser S, Tuzcu M, Guvenc M, Cetintas B, Irtegun S, Tastan H, Sahin K (2009) A practical HPLC method to measure reduced (GSH) and oxidized (GSSG) glutathione concentrations in animal tissues. *J Anim Vet Adv* 8(2):343–347
- Zhu F, Cheng QY, Xue SG, Li CX, Hartley W, Wu C, Tian T (2018) Influence of natural regeneration on fractal features of residue microaggregates in bauxite residue disposal areas. *Land Degrad Dev* 29(1):138–149. <https://doi.org/10.1002/ldr.2848>